Supporting Information

Development of a Physiologically Based Pharmacokinetic (PBPK) Model for F-53B in Pregnant Mice and Extrapolation to Humans

Jing Zhang[a], Shen-pan Li[a], Qing-Qing Li[b], Yun-Ting Zhang[a], Guang-Hui Dong[a], Alexa Canchola[c,d], Xiaowen Zeng[a*], Wei-Chun Chou[c,d*]

[a] Joint International Research Laboratory of Environment and Health, Ministry of Education, Guangdong Provincial Engineering Technology Research Center of Environmental Pollution and Health Risk Assessment, Department of Occupational and Environmental Health, School of Public Health, Sun Yat-sen University, Guangzhou, China

[b] Acacia Lab for Implementation Science, Institute for Global Health, Dermatology Hospital of Southern Medical University, Guangzhou, China

[c] Department of Environmental Sciences, University of California, Riverside, California 92521, United States

[d] Environmental Toxicology Graduate Program, University of California, Riverside, CA 92521, United States

***Corresponding authors**: Wei-Chun Chou (weichunc.chou@ucr.edu); Xiao-Wen Zeng (zxw63@mail.sysu.edu.cn)

Pages: 40

Figures: 4

Tables: 13

S1. Dose Setting

The calculation of the F-53B dose was based on our previous article[1]. Briefly, oral dose = Human Equivalent Dose (HED) × Uncertainty Factor for Human (UFH) × Uncertainty Factor for Interspecies (UFI) × Uncertainty Factor for Toxicokinetics (UFT)[2]. Due to the lack of pharmacokinetic data for F-53B, the volume of distribution from the PBPK model for perfluorooctane sulfonate (PFOS) was used[3]. Where HED = average serum concentration (μg/mL) * clearance (CL; mL/kg/day). CL = a volume of distribution (Vd) × (ln (2) ÷ half-life ($t_{1/2}$)); Vd: 0.23 L/kg and 0.268 L/kg for human and mice, respectively; $t_{1/2}$: 15.3 years × 365 days/year and 36.9 days for human and mice, respectively. UFH: a correction factor of 10×. UFI: a correction factor of 3×. UFT = CL_{mice}/ CL_{human} (a correction factor of 176.6 ×). Based on the general adult (4.78 ng/mL)[4] and occupational people (102.3 ng/mL)[5] plasma concentration, an equivalent dose of 0.72 and 15.45 μg/kg was defined. Our preliminary experiment at exposure doses of 0.8, 8 and 80 μg/kg showed that no toxic effects were observed in pregnant mice. In order to ensure that F-53B could be detected in both pregnant mice and fetus throughout the whole experimental period, we finally set the exposure dose at 80 μg/kg.

S2. Sample Pretreatment and Detection

S2.1 Toxicokinetic study in mice

Eighty C57BL/6J female and male mice were obtained from Medical Laboratory Animal Center of Guangdong and mated in a ratio of 1:1. Pregnant mice confirmed by vaginal plug examination were subjected to a 12 h/12 h light/dark cycle with food and water available ad libitum. All the animal treatments were approved by the ethics committee of Sun Yat-Sen University (SYSU-IACUC-2022-001602). Pregnant mice were randomly divided into two groups and administered with 80 μg/kg BW of F-53B by oral (n=20) or lateral tail vein injection (n=20) on gestation day (GD) 13. Dose setting was set as previously described. For the toxicokinetic study, samples of maternal plasma, maternal liver, fetal brain, fetal liver, placenta and urine and feces were

collected throughout the experimental period (GD13-GD17), and samples of fat, amniotic fluid, maternal brain, heart, spleen and other were collected on the end of the experiment (GD17). At 2, 4, 8, 12, 24, 48, and 96h after administration, whole blood was taken from the ophthalmic veins after anesthesia via isoflurane and placed in sodium heparin anticoagulation tubes. Animals were subsequently euthanized by cervical dislocation and their organ tissues were collected. In addition, at 0.5, 36, and 72 h, only blood was collected without execution. Urine and fecal samples were collected at regular intervals (i.e., 0, 0-2, 2-4, 4-8, 8-12, 12-24, 24-36, 36-48, 48-72, 72-96h after administration) and recorded the quality. Detailed experimental arrangements and sample descriptions are shown in Table 1. The samples were frozen at -80 °C before analysis. F-53B content was detected by ultraperformance liquid chromatography attached to an Agilent 6410B Triple Quadrupole tandem mass spectrometer (Palo Alto and Santa Clara, CA USA), and protein binding assay was determined by ultrafiltration centrifugation.

S2.2 Sample extraction

F-53B standards and other reagents were described in Table S1-S2. Sample preparation and analytical methods have been reported in our previous articles[1,6]. Use 0.1 mL of liquid biological sample in mixed with 2 mL of 0.1 M formic acid followed by 25 μL of isotopically labeled internal standard mixture (20 ppb). The Waters Oasis HLB solid phase extraction cartridge was activated with 2 mL methanol with 2 mL 0.1 M formic acid, and then the prepared liquid biological sample was loaded onto the column and washed sequentially with 3 mL 0.1 M formic acid, 6 mL 50% 0.1 M formic acid/50% methanol, and 1 mL 1% ammonia. The cartridge was dried under vacuum. Then, 2 mL of 1% ammonia acetonitrile was added for elution. Finally, the eluate was sequentially centrifuged at 4500 rpm, 4 °C for 1 min and evaporated to near dryness under a stream of high-purity nitrogen at 40 °C. The cartridge was washed with 70 μL of methanol and 30 μL of 30 μM ammonia. The samples were reconstituted with 70 μL methanol and

30 μL 20 mM ammonium formate. The extracts were then transferred to polypropylene centrifuge tubes and centrifuged at 12,000 rpm, 4 °C for 10 min. Twenty-five microliters of supernatant was transferred to a polypropylene autosampler vial for UHPLC-MS/MS analysis. For solid biological samples, about 10 mg of tissue was clipped and recorded the mass. 200 μL of acetonitrile was added and ground into a homogenate using a tissue grinder, then 800 μL of acetonitrile was added, vortexed and shaken to mix and instantaneously centrifuged. Sonication for 30 minutes, centrifugation at 12000rpm, 4 °C for 10 min, take around 0.2 mL of supernatant for pre-treatment, the rest of the method is the same as above.

S2.3 Chromatography-Mass Spectrometry

The target analytes were separated and quantified using an ultraperformance liquid chromatography attached to an Agilent 6410B Triple Quadrupole tandem mass spectrometer (Palo Alto and Santa Clara, CA USA).

Chromatographic conditions: An Ascentis Express F5 Column was used and the column temperature was maintained at 40 °C. The mobile phase consisted of 20 mM ammonium formate (solvent A) and 100% methanol (solvent B), and the flow rate was maintained at 0.3 mL/min. The program was started from 55% A and 45% B, held for 6 min, increased to 95% B and returned to the initial state after a 1-min hold, and the column was equilibrated for a further 3 min.

Mass spectrometry conditions: Electrospray ionization (ESI) was used for ionization. The desolventization temperature was set at 350 °C, and the dissociation voltage and collision energy were limited to the range of 58-165 V and 3-60 eV, respectively. The results were recorded by multiple reaction monitoring (MRM).

S2.4 Quality Control

F-53B concentrations in the samples were obtained using an internal standard method. Nine calibration curve points were used, between 0.05 and 100 ng/mL, and the

coefficient of determination (R^2) for each calibration was higher than 0.99. Sample recoveries were all between 80 % and 120 %. Between every 10 samples, a blank (calf serum) was inserted to monitor possible contamination in sample extraction. A solvent blank (70 % methanol) and a set of standard curves were set up every 20 samples to detect instrumental background values and instrumental response and drift. The limit of detection (LOD) of the target compounds was defined as the lowest detected concentration in the sample with a signal-to-noise ratio of 3 (S/N = 3), and concentration values below the LOD will be replaced by LOD /√2. The limit of quantification (LOQ) of the target compounds was defined as the lowest detected concentration in the sample with a signal-to-noise ratio of 10 (S/N = 10). The materials used in the experiments were soaked in methanol for more than 4 h to minimize any background effects.

S3. Protein Binding Assay

Protein binding of F-53B in the plasma of pregnant mice as determined by ultrafiltration centrifugation[7]. Plasma was centrifuged using the 10 kDa ultrafiltration centrifuge tube to filter out plasma proteins with molecular weights >10 kDa (recovery of 80%). Centrifuged plasma was determined F-53B concentration by UHPLC-MS/MS as described above. Protein binding ratio was calculated based on the total amount of F-53B in the plasma before ultrafiltration (Atotal) and the unbound amount of F-53B in the plasma after ultrafiltration (Afree)[8] (Equation S1). The free fraction of F-53B (un-bound to protein) was calculated by Equation S2.

$$Protein\ binding\ ratio\ (\%) = [(Atotal - Afree)\ /\ Atotal] \times 100\% \qquad \text{(S1)}$$

$$Free = (1 - Protein\ binding\ ratio)\ /\ 100\% \qquad \text{(S2)}$$

S4. Equations and Codes for the Pregnancy PBPK model

S4.1 Two-compartment gastrointestinal (GI) model

A two-compartment gastrointestinal model was used to describe the absorption process

of F-53B after oral administration/exposure. Briefly, F-53B enters the stomach via oral administration and subsequently enters the small intestine at the gastric emptying rate (*GE*; per hour). The first-order constants *K0* (per hour) and *Kabs* (per hour) were used to characterize the absorption of F-53B in the stomach and small intestine. Through the portal vein, F-53B is transported directly from the GI tract to the liver. The equations describing oral uptake are provided and explained below:

$$RST = -K0 \times AST - GE \times AST \quad \text{(S3)}$$

$$RSI = GE \times AST - Kabs \times ASI - Kunabs \times ASI \quad \text{(S4)}$$

$$RabsSI = Kabs \times ASI \quad \text{(S5)}$$

Where *RST*, *RSI*, and *RabsSI* are the rates of change in F-53B amounts in the stomach, small intestine, and small intestinal transport from the portal vein to the liver (milligrams per hour), respectively; *AST* and *ASI* are the amounts of F-53B in the stomach and small intestine (milligrams), respectively; *Kunabs* is the rate constant for excretion of unabsorbed F-53B via the feces (per hour).

S4.2 Renal reabsorption and filtration

The kidney was described as a three-compartment model: a) proximal tubular lumen/filtrate, b) proximal tubular cells (PTCs), and c) the rest of the kidney (Figure 1). The kidney influences F-53B content in plasma mainly through glomerular filtration rate (GFR) and tubular reabsorption and excretion. And the renal reabsorption was described by the Michaelis-Menten equation[9]. The Michaelis-Menten parameter, based on in vitro to in vivo extrapolation, has been used to characterize the active transport of PFOS mediated in proximal renal tubular cells via the basolateral and apical organic anion transporters Oat1 and Oat3. Due to the lack of parameters to describe renal reabsorption for F-53B, in this study, initial parameters values were assumed to be the same as the result in the rat PFOS PBPK model. The kidney filtration and reabsorption are described by Equations S6-S11:

$$RA\_baso = (Vmax\_baso \times CKb) / (Km\_baso + CKb) \quad \text{(S6)}$$

$$RA\_apical = (Vmax\_apical \times CFil) / (Km\_apical + CFil) \quad \text{(S7)}$$

$$RPTC = Rdif + RA\_apical + RA\_baso - RAefflux \quad \text{(S8)}$$

$$RKb = QK \times (CPlas - CVK) \times Free - RCI - Rdif - RA\_baso \quad \text{(S9)}$$

$$RCI = CPlas * GFR * Free \quad \text{(S10)}$$

$$Rdif = Kdif \times (CKb - CPTC) \quad \text{(S11)}$$

Where *RA_baso* and *RA_apical* are the rates of transport of F-53B from the kidney plasma to the PTCs via the basolateral transporter and apical transporter (milligrams per hour), respectively, and the process were described by Michaelis-Menten equations. *RPTC* and *RKb* are the rates of change in F-53B amounts in PTCs and renal blood (milligrams per hour), respectively; *RCl* is the clearance rate of F-53B via the GFR (milligrams per hour); *Rdif* is the diffusion rate from the kidney to the PTCs (milligrams per hour); *RAefflux* is the efflux rate of F-53B from PTCs back into plasma (milligrams per hour). *CKb* and *CFil* are the concentration of F-53B in the renal blood and filtrate compartment (milligrams per litre), respectively. *Kdif* is the diffusion rate from PTCs to renal blood (litre per hour).

S4.3 Elimination

The first-order constant *Kurine* (per hour) was used to characterize the urinary excretion of F-53B from the filtrate compartment. The first-order constant *Kbile* (per hour) was used to characterize the biliary excretion of F-53B and co-excretion through the feces with the unabsorbed portion of the intestine. Equations as shown below:

$$Rurine = Kurine \times AFil \quad \text{(S12)}$$

$$Rfeces = Kbile \times AL + Kunabs \times ASI \quad \text{(S13)}$$

Where *Rurine* and *Rfeces* are the urine and fecal elimination rates of F-53B (milligrams per hour), respectively; *Kurine* and *Kbile* are the urine and biliary excretion rate constant of F-53B (litre per hour), respectively; *AFil* is the amount of F-53B in the filtrate compartment (milligrams); *AL* is the amount of F-53B in the liver (milligrams).

S4.4 Mass balance equations in flow-limited compartments

Tissues of the model are assumed as flow-limited compartments besides amniotic fluid (Figure 1), and only the free fraction of F-53B (un-bound to plasma proteins, Equation S2) were able to in and out of each compartment. Fat compartment was used as example and the equations are listed below:

$$RF = QF\_P \times (CPlas - CVF) \times Free \quad \text{(S14)}$$

$$CVF = CF / PF \quad \text{(S15)}$$

Where *RF* is the rate of change in F-53B amounts in the fat (milligrams per hour); *QF_P* is the volume of blood flow to fat tissue per hour (litre per hour), and described as a growth equation reflecting the dynamic changes during pregnancy (Tables S5 – S6); *CPlas* is the concentration of F-53B in the maternal plasma (milligrams per litre); *CVF* is the concentration of F-53B in the plasma leaving fat tissue (milligrams per litre); *Free* is the free fraction of F-53B in plasma (unitless); *CF* is the F-53B concentration in fat tissue (milligrams per litre); *PF* is the fat-to-plasma partition coefficient (unitless).

S4.5 Bidirectional diffusion process

Fetus exposures to F-53B only via placental transfer, and the excretion is also via placenta and back into the maternal circulation. Using bidirectional diffusion process with first-order rate constants (Ktrans1, Ktrans2, Ktrans3, and Ktrans4, litre per hour) to characterize the transfer of F-53B between the placenta and fetal plasma / the rest of the fetal body and the amniotic fluid compartment. Equations are listed below:

$$Rtrans\_1 = Ktrans\_1 \times CVPla \times Free \quad \text{(S16)}$$

$$Rtrans\_2 = Ktrans\_2 \times CPlas\_Fet \times Free \quad \text{(S17)}$$

$$Rtrans\_3 = Ktrans\_3 \times CVRest\_Fet \times Free\_Fet \quad \text{(S18)}$$

$$Rtrans\_4 = Ktrans\_4 \times CAm \quad \text{(S19)}$$

Where *Rtrans1* and *Rtrans2* are the placenta transfer rates of F-53B from maternal plasma to fetal plasma and from the fetal plasma back to maternal plasma (milligrams per hour), respectively; *Rtrans3* and *Rtrans4* are the transfer rates of F-53B from the amniotic fluid to the rest of fetal body, and from the rest of fetal body to the amniotic

fluid (milligrams per hour), respectively. *CVPla* and *CAm* are the F-53B concentration in the placenta and amniotic fluid (milligrams per litre), respectively; *CPlas_Fet* and *CVRest_Fet* are the F-53B concentration in the fetal plasma and fetal rest of body (milligrams per litre), respectively. *Free_Fet* is the free fraction of F-53B in fetal plasma (unitless).

S5. Calculation of Chemical-Specific Parameters

Maternal partition coefficients (*PCs*) values are the ratio of the area under the curve (AUC) of the tissue to the plasma of F-53B (unitless). As fetal mice were unable to collect cord blood, the *PCs* for fetal mice were assumed to the ratio of the AUC of the tissue to the placenta. When lack of continuous concentration data, the *PCs* for mice estimated in the PFOS PBPK model[10,11] were used as initial values. Equations are listed below:

$$PC = AUC_{tissue} / AUC_{plasma} \quad \text{(S20)}$$

$$PC\_Fet = AUC_{tissue\_Fet} / AUC_{placenta} \quad \text{(S21)}$$

Where *PC* and *PC_Fet* are partition coefficients of mother and fetus (unitless), respectively; AUC_{tissue}, AUC_{plasma}, AUC_{tissue_Fet} and $AUC_{placenta}$ are area under the curve of maternal tissue, maternal plasma, fetal tissue and placenta (hour×milligrams per litre), respectively.

Absorption and elimination parameters were calculated with a one-compartment toxicokinetic model using in-house experimental data with the built-in pharmacokinetic model of Phoenix WinNonlin® software (version 8.1, Pharsight, Certara®™ Company, Princeton, NJ, USA). The one-compartment toxicokinetic model assumes that the body consists of a single compartment and compounds are uniformly distributed immediately upon entry. The first-order constants *kabs* (per hour) and *kelim* (per hour) are used to characterize the gastrointestinal tract absorption and elimination[12]. Equations as shown below:

$$\frac{dC}{dt} = Kabs \times \frac{D}{Vd} - Kelim \times C \quad \text{(S22)}$$

$$\frac{dAGI}{dt} = -Kabs \times D \quad \text{(S23)}$$

Where *D* is the dose into the gastrointestinal tract (milligrams per kilogram); *C* is the F-53B concentration in the plasma (milligrams per litre); *AGI* is the F-53B amount in gastrointestinal tract (milligrams); *Vd* is the volume of distribution (litre per kilogram).

S6. Toxicokinetic Parameters

Tissue distribution studies were calculated by normalized sample concentration (pmol/g BW) taken at 96 h after oral and IV exposure of F-53B[13]. Absolute bioavailability was calculated as the ratio of AUC_{plasma} from oral to IV exposure to F-53B[14]. Pharmacokinetic (PK) parameters were calculated by noncompartmental method built-in Phoenix WinNonlin® software. The half-life ($t_{1/2}$) and the AUC from 0 to infinity ($AUC_{0-\infty}$) were calculated as equations below:

$$t_{1/2} = \ln(2) / Lz \quad \text{(S24)}$$

$$\mathrm{AUC}_{0-\infty} = \mathrm{AUC}_{0-t} + \frac{C_t}{Lz} \quad \text{(S25)}$$

where *lz* is the first-order rate constant obtained from the terminal (log-linear) portion of the time-concentration curve (per hour). The C_t and AUC_{0-t} were the concentration (milligrams per litre) and area under the curve at last measurable time (hour×milligrams per litre).

S7. Sensitivity Analysis

A local sensitivity analysis was performed on the gestational model for F-53B in mice and humans to determine which model parameters had high impacts on the area under the curve (AUC) of maternal (plasma, liver, placenta) and fetal (plasma, liver, brain). This analysis was conducted by varying each parameter by 1% of the original value and then examining the effect on the output of the selected model by calculating the normalized sensitivity coefficient (NSC)[15], the equation as shown below:

$$\mathrm{NSC} = \frac{\Delta \mathrm{r}}{\mathrm{r}} \times \frac{\mathrm{p}}{\Delta \mathrm{p}} \quad \text{(S26)}$$

Where r is the response variable; Δr is the change of the response variable resulting from 1% increase in the parameter value; p is the original value of the parameter of interest; and Δp is 1% of the original value of the parameter. An absolute value of NSC ≥ 30% indicates the parameter influences the response variable[11].

For sensitivity analysis involving time-varying parameters, the value of p used in Equation S26 was the original value of the baseline parameter (e.g., BW0 in body weight growth function [Table S5]) and Δp is 1% of the original value of the baseline parameter. This approach allowed us to assess the overall impact of changes in the time-varying parameter on the model outcomes. Each 1% increase in the baseline parameter values was represented by the following equation:

$$g_{new} = g \times 1.01 \quad \text{(S27)}$$

where g_{new} is the baseline parameter with 1% increase, and g is the original baseline parameter value.

S8. Monte Carlo Simulations

Monte Carlo analyses were applied to pregnancy PBPK models of humans to characterize uncertainty and inter-individual variability of parameters on model output. Influential parameters (i.e., parameters with NSC values ≥ 30%) identified in the local sensitivity analyses, along with calibration parameter values, were included in the Monte Carlo analyses, with their mean values considered as the central tendency of the distributions. The parameter values were then randomly sampled based on predefined probability distributions from previous studies[16]. Each parameter distribution was truncated at the 2.5th and 97.5th percentiles to establish the upper and lower bounds (Tables S9). Table S9 lists these parameters with high sensitivity coefficients, including physiological parameters (e.g., BW) and chemical-specific parameters (e.g., PRest, Free, Ktrans 1C, Ktrans 2C, and Free_Fet). Physiological parameters were all assumed to be normally distributed, and the partition coefficients, rate constants, and other chemical-specific parameters were assumed to be lognormally distributed. The default

coefficient of variation (CV) for the partition coefficients was 20%, whereas the CVs for the physiological parameters and other chemical specificity parameters were 30%. For parameters described by equations reflecting changes during gestation (i.e., Growth parameters), the variation was randomly sampled from a normal distribution with a CV of 20%.

Growth parameters were expressed as a baseline value plus with the incremental change. For example, the equation for body weight listed in Table S5 is *BW = BW0 + Increased tissue volumes during gestation* (Table S5). In this equation, BW0 is the baseline value. During Monte Carlo sampling, baseline values were drawn from a predefined distribution based on empirical data. As the simulation progressed, the baseline values were randomly sampled and dynamically updated according to the predefined growth equations that reflect realistic physiological changes during pregnancy. This approach ensured that parameters varied over time and characterized population variability.

Due to the absence of detailed historical exposure information for different pregnancy populations, and to address the uncertainty and variability associated with unspecified exposures, we used previously described EDIs to obtain simulated values from human prepregnant and gestational PBPK modeling and compared the results with the concentrations of F-53B in maternal plasma and cord blood measured in published studies. Table S10 shows details of the human biomonitoring data used for the comparison. For human exposure scenarios, we assumed that women become pregnant at age 30 years. We simulated exposures from birth to age 30 years and from age 30 years onwards, including the 38 weeks of pregnancy (the collection time point for most biomonitoring datasets), at a constant dose of these exposures. The trajectory of time-varying parameters before and after pregnancy was kept constant except for physiological changes during pregnancy, which were described using time-varying parameters (Table S6). Predictions were derived and compared with measured data.

S9. Supplementary Tables

Table S1

Target analytes information**.**

Acronym	CAS Number	Molecular Formula	Molecular Weight	Structure
F-53B	73606-19-6	$C_8ClF_{16}KO_4S$	570.67 g/mol	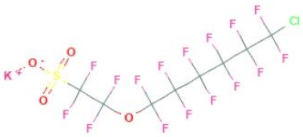

Table S2

Instruments and Reagents information**.**

Instruments and Reagents	Manufacturer
Agilent 1200 ultraperformance liquid chromatography -Connected with 6410B Triple Quadrupole tandem mass spectrometer	Agilent Technologies，USA
Chromatography columns (Ascentis Express F5 PFP)	Sigma–Aldrich，USA
Chromatography guard columns (Ascentis Express F5 PFP)	Sigma–Aldrich，USA
Tissue grinder OSE-Y30	TIANGEN Biotech，China
Nitrogen blowtorch	Orgnomation，USA
Ultrapure water meter	Millipore，USA
Waters Oasis HLB-Solid phase extraction column	Waters，USA
Methanol (HPLC grade)	Honeywell，USA
Acetonitrile (HPLC grade)	Honeywell，USA
Ammonia (liquid, 29%)	Sigma-aldrich，USA
Methanoic acid (purity ≥98%)	Sigma-aldrich，USA
Ammonium formate (purity ≥99.0%)	Sigma-aldrich，USA
Fetal calf serum	SiJiQing Co., Ltd，China

Isopropanol (Guaranteed reagent)	GuoAo Co., Ltd，China
F-53B (purity ≥97%)	Jianglaibio Co., Ltd，China
Tween 20 (purity ≥98%)	Sigma-aldrich，USA
Saline (Medicine)	XinRan Biotech，China
Ultrafiltration tube (0.5ml 10K)	Merck millipore，USA

Table S3

Model parameters description of gestational PBPK model of mice and humans

Symbols	Unit	Description
BW	Kg	Body weight
Free	Unitless	Free fraction of F-53B in maternal plasma
Free_Fet	Unitless	Free fraction of F-53B in fetal plasma
GEC	$1/h/BW^{0.25}$	Gastric emptying rate constant
GFRC	L/h/kg kidney	Glomerular filtration rate constant
Htc	Unitless	Hematocrit
K0C	$1/h/BW^{0.25}$	Rate constant of absorption of F-53B in stomach
KabsC	$1/h/BW^{0.25}$	Rate constant of absorption of F-53B in small intestine
KbileC	$1/h/BW^{0.25}$	Biliary elimination rate constant
Kdif	L/h	Diffusion rate from proximal tubule cells (PTCs) to kidney serum
KeffluxC	$1/h/BW^{0.25}$	Rate constant of clearance of F-53B from PTCs into blood
Km_apical	mg/L	The Michaelis constant (Km) of apical transporters
Km_baso	mg/L	The Michaelis constant (Km) of basolateral transporters
Ktrans1C	$L/h/kg^{0.75}$	Mother-to-fetus placental transfer rate constant
Ktrans2C	$L/h/kg^{0.75}$	Fetus-to-mother placental transfer rate constant
Ktrans3C	$L/h/kg^{0.75}$	Fetus-to-amniotic fluid transfer rate constant
Ktrans4C	$L/h/kg^{0.75}$	Amniotic fluid-to-fetus transfer rate constant
KunabsC	$1/h/BW^{0.25}$	Rate constant of unabsorbed F-53B dose to appear in feces
KurineC	$1/h/BW^{0.25}$	Urinary elimination rate constant
N	Unitless	Number of fetus
PB_Fet	Unitless	Brain-to-plasma partition coefficient
PF	Unitless	Fat-to-plasma partition coefficient
PK	Unitless	Kidney-to-plasma partition coefficient
PL	Unitless	Liver-to-plasma partition coefficient
PL_Fet	Unitless	Liver-to-plasma partition coefficient for fetuses
PM	Unitless	Mammary gland-to-plasma partition coefficient
PPla	Unitless	Placenta-to-plasma partition coefficient

PRest	Unitless	Rest of body-to-plasma partition coefficient
PRest_Fet	Unitless	Rest of body-to-plasma partition coefficient for fetuses
protein	mg protein/PTCs	Amount of protein in proximal tubule cells
QBC_Fet	Unitless	Fractional blood flow to fetal brain
QCC	$L/h/kg^{0.75}$	Cardiac output scalar
QFC	Unitless	Fractional blood flow to Fat (%QC)
QKC	Unitless	Fractional blood flow to kidney (%QC)
QLC	Unitless	Fractional blood flow to liver (%QC)
QLC_Fet	Unitless	Fractional blood flows to fetal liver
QMC	Unitless	Fractional blood flow to mammary gland (%QC)
QPla	L/h	Blood flow to placenta
RAFapi	Unitless	Relative activity factor for apical transporters
RAFbaso	Unitless	Relative activity factor for basolateral transporters
VAm	L	Amniotic fluid volume
VAmX	L/one fetus	Amniotic fluid volume for one fetus
VFC	Unitless	Fraction of fat tissue (%BW)
VFet1	L	Fetus volume for one fetus (mice)
VFilC	L/kg BW	Fraction of filtrate (10% of kidney volume)
VKC	Unitless	Fraction of kidney tissue (%BW)
VL_Fet	L	Volume of liver tissue for the fetus (rats)
VLC	Unitless	Fraction of liver tissue (%BW)
VLC_Fet	Unitless	Fractional liver tissue for fetuses
Vmax_apical_invitro	pmol/mg protein/min	Vmax of apical transporters
Vmax_baso_invitro	pmol/mg protein/min	Vmax of basolateral transporters
VMC	Unitless	Fraction of mammary tissue (%BW)
VPla	L	Volume of placenta
VPlasC	Unitless	Fraction of plasma volume (%BW)
VPlasC_Fet	Unitless	Fraction volume of fetal plasma
VPTCC	L/kg kidney	Volume of proximal tubule cells
VRest_Fet	L	Volume of rest of body for fetuses

Table S4

Physiological parameters for prepregnant humans and pregnant mice or humans used in the PBPK model.

Symbols	Unit	Mice		Human		
		Pregnant	References	prepregnant	Pregnant	References
BW	Kg	0.025	In-house experiment	54	60	Haddad et al. (2001)[17]
GEC	1/h/BW0.25	0.54	Yang et al. (2013)[18], Chou and Lin (2019)[10]	3.51	3.51	Yang et al. (2015)[19]
GFRC	L/h/kg kidney	59	Qi et al. (2004)[20], Chou and Lin (2019)[10]	27.28	equ[a]	Worley et al. (2017)[16]
Htc	Unitless	0.48	Hejtmancik et al. (2002)[21], Chou and Lin (2019)[10]	0.44	equ[a]	Davies and Morris et al. (1993)[22]
protein	mg protein/PTCs	2.00E-06	Addis et al. (1936)[23], Hsu et al. (2014)[24]	2.00E-06	2.00E-06	Addis et al. (1936)[23]
Tissue volume (fraction of BW)						
VFC	Unitless	0.068	Brown et al. (1997)[25]	0.214	0.214	Loccisano et al. (2012)[26], Yoon et al. (2009)[27]
VFilC	L/kg BW	0.0017	Worley and Fisher (2015)[9]	0.00084	0.00084	Worley et al. (2017)[16]
VKC	Unitless	0.017	Brown et al. (1997)[25]	0.004	0.004	Brown et al. (1997)[25]

VLC	Unitless	0.055	Brown et al. (1997)[25]	0.026	0.026	Brown et al. (1997)[25]
VMC[b]	Unitless	0.01	Hanwell and Linzell (1973)[28]	0.0062	0.0062	Loccisano et al. (2012)[26], Yoon et al. (2009)[27]
VPlasC	Unitless	0.049	Brown et al. (1997)[25]	0.0428	0.0428	Worley et al. (2017)[16]
VPTCC	L/kg kidney	1.35E-04	Addis et al. (1936), Hsu et al. (2014)[24]	1.35E-04	1.35E-04	Hsu et al. (2014)[24]
Tissue blood flows (fraction of QC)						
QCC	L/h/kg0.75	16.5	Brown et al. (1997)[25]	16.4	16.4	Yoon et al. (2011) [35]
QFC[b]	Unitless	0.07	Brown et al. (1997)[25]	0.052	0.052	Yoon et al. (2011)[29]
QKC	Unitless	0.091	Brown et al. (1997)[25]	0.175	0.175	Brown et al. (1997)[25]
QLC	Unitless	0.161	Brown et al. (1997)[25]	0.25	0.25	Brown et al. (1997)[25]
QMC	Unitless	0.002	Hanwell and Linzell (1973)[28]	0.027	0.027	Yoon et al. (2011)[29]
Fetal parameters						
QBC_Fet	Unitless	0.1055	Carter, A. M. and W. Gu (1988)[30], Yoon (2009)[27]	—	0.19	Kapraun et al. (2019)[31]
QLC_Fet	Unitless	0.161	Value was assumed to be same as the mother	—	equ[a]	Kapraun et al. (2019)[31]

N	Unitless	8	In-house experiment	—	—	
VPlasC_Fet	Unitless	0.049	Value was assumed to be same as the mother	—	0.0428	Value was assumed to be same as the mother

[a] equ means parameter was calculated from the growth equation (Tables S5-S6).
[b] Parameters of rat were used instead of mice; All abbreviations are defined in Table S1.

Table S5

Equations for describing changes in physiological parameters for pregnant mice and their fetus

Parameters	Equations	References
Pregnant mice		
Body weight (BW, kg)	BW = BW0[a] + Increased tissue volumes during gestation[b]	O'Flaherty et al. 1992[32]
	BW0=20.8	In-house experiment
Cardiac output index (QC, L/d)	QC = QC0 + N*(QDEC1 + QDEC2 +QCAP)*(1–Htc)	O'Flaherty et al. 1992[32], Clarke et al. 1993[33]
	QC0 = QCC*($BW^{0.75}$)*(1–Htc)	
	GD[c]5.5-9.25: QDECl = QPla	
	GD9.25-11: QDEC2 = 2.2*exp(-0.23*(GD – 9.25)).	
	GD > 11: QCAP = 0.1207*(GD – 11))[4.36]	
Tissue volume (L, actual volume, changing during pregnancy)		

Volume of mammary gland (VM)[d]	VM0 = 0.01*BW0	Crowell et al.2013[34]
	VM = VM0*(1 + 0.27*GD*(BW_{mice}/BW_{rat}))	O'Flaherty et al. 1992[32], O'Flaherty et al. 1995[35], Ward et al. 1997[36]
Volume of fat (VF)[d]	VF0 = 0.07*BW0	Crowell et al.2013[34]
	VF = VF0*(1 + 0.0165 *GD *(BW_{mice}/BW_{rat}))	O'Flaherty et al. 1992[32], O'Flaherty et al. 1995[35]
Placenta (VPla, for a whole litter)	VPla = (VEC1 + VEC2 + VCAP)/10^6	O'Flaherty et al. 1992[32], Clarke et al. 1993[33]
	GD0-6: VPla = 0;	
	GD6-9.25: VEC1 = N*8*(GD – 6)	
	GD9.25-19.5: VEC2 = N*32*exp(-0.23*(GD – 9.25)) ,	
	VCAP = N*40*(exp(0.28*(GD – 9.25)) – 1)	
Rest of body (VRest)	VRest = 0.93*BW – VL – VK – VM – VF – VPla – VFet – VAm	
Tissue blood flow (L/h, actual flow changing during pregnancy)		
Mammary gland (QM)	QM = QM*(VM/VM0)*QC	Crowell et al.2013[34]
Fat (QF)	QF = QF*(VF/VF0)*QC	Crowell et al.2013[34]
Placenta (QPla, for a whole litter)	QPla_Fet = (0.02*QDEC + QCAP)*N/12	O'Flaherty et al. 1992[32], Clarke et al. 1993[33]
	QPla = ((N* QPla_Fet) /24) *(1–Htc)	
Rest of body (QRest)	QRest = QC – QL – QK – QF - QM – QPla	

Fetus		
Body weight for individual fetus (VFet_1, kg)	VFet_1 = VEF 1 + VEF2 + VEF3. GD0-8.6: VEF1 = $(0.12*GD)^{4.53}/10^6$ GD8.6-15.8: VEF2 = $(1.2*(GD-8.6))^{2.6}/10^6$ GD15.8-19: VEF3 = $(((1250-(1.2*(GD-8.6))^{2.6})/3.2)*(GD-15.8))/10^6$	O'Flaherty et al. 1995[35]
Body weight for whole fetus (VFet, kg)	VFet = VFet_1*N	O'Flaherty et al. 1995[35]
Cardiac output (QC_Fet, L/h)	QEF = (QPla/(1 + 20,000 *exp(-0.55 *GD)))	O'Flaherty et al. 1992[32]
Amniotic fluid volume (VAm, L)[d]	GD >= 8: VAm = $((-4e^{-6})*GD^3 + 0.0002*GD^2 - 0.0023*GD + 0.0099)*(BW_{mice}/BW_{rat})$	Clewell et al. 2008[37], Loccisano et al. 2012[26], Wykoff 1971[38]
Volume of fetal liver (VL_Fet, L)	VL_Fet = (0.406/(1 + exp((14.716 – GD)/0.907))/1000)	In-house experiment
Volume of fetal brain (VB_Fet, L)[d]	VB_Fet = (4.191*exp(-exp(2.554 – 0.06726*GD))/1000)*N*(BWmice/BWrat)	Sikov, M. R. and J. M. Thomas (1970)[39], Yoon (2009)[27]
Rest of body for fetuses (VRest_Fet)	VRest_Fet = 0.93*VFet – VPlas_Fet – VL_Fet	

[a] "0" indicates parameter values on GD0 or for nonpregnant female mice.

[b] These tissues include mammary gland, fat, placenta and fetuses.

[c] GD represent gestational day (days).

[d] Correction of rat parameters by weight.

Table S6

Equations for describing changes in physiological parameters for pregnant women and fetus

Parameters	Equations	References
Pregnant woman		
Body weight (BW, kg)	BW = BW0[a] + Increased tissue volumes during gestation [b]	Loccisano et al. 2013[40], Yoon et al. 2011[29]
Cardiac output index (QCI, L/h/kg)	$QC = QC0 + 3.2512*GA^{c} + 0.15947*GA^{2} – 0.0047059* GA^{3}$	Abduljalil et al. 2012[41], Kapraun et al. 2019[31]
	$QC0 = QCC*BW^{0.75}*(1–Htc)$	
Glomerular filtration rate (GFR, L/h)	$GFR = (113.73 + 3.5784*GA - 0.067272*GA^{2})*(0.06)$	Abduljalil et al. 2012[41], Kapraun et al. 2019[31]
Hematocrit (Htc, Unitless)	$Htc = (39.192 - 0.10562*GA - (7.1045e^{-4})*GA^{2}))/100$	Abduljalil et al. 2012[41], Kapraun et al. 2019[31]
Tissue volume (L, actual volume, changing during pregnancy)		
Mammary gland (VM, L)	VM = BW*(((VMC + (0.0065*exp(-7.444868*exp(-0.000678*(GA*198)))))))	Gentry et al. 2003[42], Loccisano et al. 2013[40], Yoon et al.2011[29]
Fat (VF, L)	VF = (1/0.95)*(17.067 + 0.14937*GA)	Abduljalil et al. 2012[41], Kapraun et al. 2019[31]
Plasma (VPlas, L)	VPlas = (1.2406/(1 + exp(-0.31338*(GA – 17.813)))) + 2.4958	Abduljalil et al. 2012[41], Kapraun et al.

		2019[31]
Amniotic fluid (VAm, L)	VAm = (822.34/(1 + exp(-0.26988*(GA – 20.150))))	Abduljalil et al. 2012[41], Kapraun et al. 2019[31]
Placenta (VPla, L)	VPla = (-1.7646*GA + 0.91775*GA^2 – 0.011543*GA^3)/1000	Abduljalil et al. 2012[41], Kapraun et al. 2019[31]
Rest of body (VRest, L)	VRest = 0.93*BW–VL–VK–VM–VF–VPla–VFet–VAm	
Tissue blood flow (L/h, actual flow changing during pregnancy)		
Mammary gland (QM, L/h)	QM0 = QMC*QC0	Gentry et al. 2003[42], Loccisano et al. 2013[40], Yoon et al. 2011[29]
	QM = QM0*(VM/VM0)	
Fat (QF, L/h)	QF0 = QFC*QC0	Gentry et al. 2003[42], Loccisano et al. 2013[40], Yoon et al. 2011[29]
	QF = ((0.01)*(8.5 + (-0.0175)*GA))*QC	
Kidney (QK, L/h)	QK = (0.01)*(17 + (-0.01)*GA)* QC	Abduljalil et al. 2012[41], Kapraun et al. 2019[31]
Liver (QL, L/h)	QL = (0.01)*(27 + (-0.175)*GA)*QC	Kapraun et al. 2019[31], Valentin and Streffer 2002[43]
Placenta (QPla, L/h)	GD >3.6: QPla = (0.00022)*(GA – 3.6)*(0.4 + 0.29*GA)*QC	Gentry et al. 2003[42], Loccisano et al. 2013[40], Yoon et al. 2011[29]

Rest of body (QRest, L/h)	QRest = QC – QL – QK – QF - QM – QPla	
Fetus		
Body weight for fetus (VFet, kg)	VFet = (0.0018282*exp((15.12691)*(1–exp(-0.077577*GA))))/1000	Gentry et al. 2003[42], Loccisano et al. 2013[40], Yoon et al. 2011[29]
Cardiac output for fetus (QC_Fet, L/h)	QC_Fet = 54*VPlas_Fet*(1 – Htc_Fet)	Clewell et al. 1999[44], Loccisano et al. 2013[40], Yoon et al. 2011[29]
Hematocrit (Htc_Fet, Unitless)	Htc_Fet = (4.5061*GA –0.18487*GA^2 + 0.0026766*GA^3)/100	Kapraun et al. 2019[31]
Volume of fetal liver (VL_Fet, L)	VL_Fet = (0.0075*exp(10.68*(1–exp((-0.062)*GA))))/1050	Kapraun et al. 2019[31], Overmoyer et al. 1987[45]
Blood flow of fetal liver (QL_Fet, L)	QL_Fet = (6.5/54)*(1 – 26.5/75)*QC_Fet	Kapraun et al. 2019[31]
Volume of fetal brain (VB_Fet, L)	VB_Fet = ((0.01574*exp(10.91*(1–exp((-0.065)*GA))))/1040)/10^3	Kapraun et al. 2019[31]
Volume of fetal rest of body (VRest_Fet,L)	VRest_Fet= (0.93*VFet) – VPlas_Fet – VL_Fet – VB_Fet	

[a] "0" indicates parameter values on GD0 or for nonpregnant women.

[b] These tissues include mammary gland, fat, placenta and fetuses.

[c] GA represent gestational age (weeks).

Table S7.

Chemical parameters for the gestational PBPK models for F-53B in mice and humans.

Kapraun Parameters	Unit	Mice		Human	
		Pregnant	References	Pregnant	References
Plasma protein binding					
Free	Unitless	0.067[a]	In-house experiment	0.067[a]	from mice PBPK model
Absorption					
K0C	$1/h/BW^{0.25}$	5.42[a]	Worley and Fisher (2015)[9], Chou and Lin (2019)[10]	0.774[a]	equ[b]
KabsC	$1/h/BW^{0.25}$	2.430	In-house experiment	0.347	equ[b]
KunabsC	$1/h/BW^{0.25}$	5.400E-04	In-house experiment	7.715E-05	equ[b]
Partition coefficient					
PF	Unitless	0.29[a]	Loccisano et al. (2012)[26]	0.29[a]	from mice PBPK model
PK	Unitless	0.80	Loccisano et al. (2012)[26]	1.26	Chou and Lin (2021)[11]
PL	Unitless	2.10	In-house experiment	2.10	from mice PBPK model
PM	Unitless	0.16	Loccisano et al. (2012)[26]	0.16	Loccisano et al. (2013)[40]
PPla	Unitless	0.08[a]	In-house experiment	0.08[a]	from mice PBPK model
PRest	Unitless	0.43[a]	Chou and Lin (2019)[10]	0.43[a]	from mice PBPK model

Placental transfer and amniotic fluid transfer rate constant					
Ktrans1C	L/h/kg$^{0.75}$	1.39[a]	Chou and Lin (2021)[11]	0.199[a]	equ[b]
Ktrans2C	L/h/kg$^{0.75}$	0.60[a]	Chou and Lin (2021)[11]	0.086[a]	equ[b]
Ktrans3C	L/h/kg$^{0.75}$	0.230	Chou and Lin (2021)[11]	0.033	equ[b]
Ktrans4C	L/h/kg$^{0.75}$	0.001	Chou and Lin (2021)[11]	1.429E-04	equ[b]
Elimination					
KbileC	1/h/BW$^{0.25}$	0.00001[a]	Chou and Lin (2019)[10]	1.429E-06[a]	equ[b]
KurineC	1/h/BW$^{0.25}$	0.02[a]	In-house experiment	0.003[a]	equ[b]
Renal reabsorption parameters					
Vmax_apical_invitro	pmol/mg protein/min	1632.576[a]	Worley and Fisher (2015)[9]	51803.00	Chou and Lin (2019)[10]
Vmax_baso_invitro	pmol/mg protein/min	393.450	Worley and Fisher (2015)[9]	479.00	Chou and Lin (2019)[10]
Km_apical	mg/L	140.987[a]	Worley and Fisher (2015)[9], Chou and Lin (2019)[10]	20.10	Worley et al. (2017)[16]
Km_baso	mg/L	50.157[a]	Worley and Fisher (2015)[9], Chou and Lin (2019)[10]	64.40	Chou and Lin (2019)[10]
RAFapi	Unitless	2.810	Chou and Lin (2019)[10]	0.001	Chou and Lin (2019)[10]
RAFbaso	Unitless	3.990	Worley and Fisher (2015)[9]	1	Worley et al. (2017)[16]

Kdif	L/h	5.4E-05[a]	Chou and Lin (2019)[10]	7.715E-06[a]	equ[b]
KeffluxC	$1/h/BW^{0.25}$	5.600	Chou and Lin (2019)[10]	0.800	equ[b]
Fetal parameters					
Free_Fet	Unitless	0.076[a]	Value was assumed to be same as the mother	0.076[a]	from mice PBPK model
PB_Fet	Unitless	1.55	In-house experiment	1.55	from mice PBPK model
PL_Fet	Unitless	2.10	Value was assumed to be same as the mother	2.10	from mice PBPK model
PRest_Fet	Unitless	0.22	Value was assumed to be same as the mother	0.22	from mice PBPK model

All abbreviations are defined in Table S3.

[a] These parameters were calibrated in the present study.

[b] These parameters were converted according to Eq. 1: $K_{human} = K_{mice} * (\text{Body weight of human} \div \text{Body weight of mice})^{-0.25}$

Table S8

Population estimated daily intakes (EDIs) for F-53B

References	City/Country	EDIs (ng/kg bw/day)				
		Fish	Water	Seafood	Total Diet	Sum
Wang et al. (2021)[46]	Shijiazhuang, China	0.114	NC[a]			0.122
Jin et al. (2020)[47]	Beijing, China			0.067		0.067
Chen et al. (2022)[48]	Tianjin, China		0.01		1.86	1.87
Sun et al. (2021)[49]	Fujian, Guangdong and Zhejiang, China			0.24–0.90 (rural)		0.57
				0.33–1.26 (urban)		0.80
Wang et al. (2022)[50]	China				0.393	0.393

[a] NC: not calculated because of the value below the limits of quantification.

Table S9

Values and parameter distributions used in the Monte Carlo analysis for the Human gestational PBPK modeling

Parameter	Unit	Distribution	Mean	SD	CV	Lower bound	Upper bound	Mean_value	SD_value
BW	Kg	Normal	60	18	0.3	24.72	95.28		
PRest	Unitless	Lognormal	0.43	0.086	0.2	0.29	0.62	-0.86	0.20
Free	Unitless	Lognormal	0.067	0.0201	0.3	0.04	0.11	-2.75	0.29
Ktrans1C	$L/h/kg^{0.75}$	Lognormal	0.199	0.0597	0.3	0.11	0.34	-1.65	0.29
Ktrans2C	$L/h/kg^{0.75}$	Lognormal	0.086	0.0258	0.3	0.05	0.14	-2.52	0.29
Free_Fet	Unitless	Lognormal	0.076	0.0228	0.3	0.04	0.12	-2.70	0.29

Note: All abbreviations are defined in Table S3; Parameters were identified in the local sensitivity analyses (i.e., parameters with NSC values ≥ 30%)

Table S10

Maternal plasma and cord blood biomonitoring data

References	City[a]	Time (years)	Maternal plasma				Core blood			
			Sample size	Concentration			Sample size	Concentration		
				Q1	Median	Q3		Q1	Median	Q3
Pan et al.2017[51]	Wuhan	2014	100	1.53	1.89	2.59	100	0.6	0.8	1.13
Chen et al.2017[52]	Wuhan	2015-2016	32	NA	1.54	NA	32	NA	0.6	NA
Chu et al.2020[6]	Guangzhou	2013	372	1.22	2.41	4.69	-			
Gao et al.2019[53]	Beijing	2015-2016	106	NA	0.094	NA	90	NA	0.091	NA
Xu et al.2019[54]	Zhejiang	2016-2017	-				98	0.5	0.731	1
Cai et al.2020[55]	Maoming	2015-2018	424	0.39	0.63	1.03	424	0.17	0.32	0.49
Wang et al.2020[56]	Beijing	1998-2018	-				650	0.269	0.453	0.809
Li et al.2021[57b]	Beijing	2015-2016	84	NA	2.58	NA	84	NA	1.16	NA
Liu et al.2021[58]	Tianjin	2010-2012	480	3.43	5.48	8.52	-			
Xia et al.2022[59]	Jinan	2017-2021	-				326	NA	0.269	NA
Zheng et al.2022[60]	Mianyang	2018	60	0.346	0.592	0.91	60	0.171	0.243	0.45
Zhang et al.2022[61]	Qingyuan	2016	94	NA	1.78	NA	94	NA	0.73	NA
Cao et al.2023[62]	Wuhan	2013-2014	-				1015	0.51	0.76	1.1

Fan et al.2023[63c]	Hefei	2021-2022	135	NA	1.39	NA	135	NA	0.54	NA
Ji et al.2023[64]	Guangzhou	2021	302	0.27	0.41	0.66	302	0.35	0.58	0.98
Li et al.2023a[65]	Maoming	2015-2018	718	0.39	0.63	1.04	-			
Li et al.2023b[66]	Wuhan	2014-2015	-				908	0.52	0.76	1.1
Tian et al.2023[67]	Zhejiang	2020-2021	169	NA	2.81	NA	-			
Zhang et al.2023[68c]	Hangzhou	2011-2012	69	2.02	2.42	2.75				

[a] All cities are in China.

[b] Missing median, replace with mean.

[c] Only choose the healthy women (control group in case-control studies).

Table S11

F-53B plasma protein binding ratio (Mean ± SEM)

	Oral (n = 4)	IV (n = 4)
Atotal (pmol/g BW)[a]	15.65 ± 1.25	25.47 ± 6.45
Afree (pmol/g BW)[b]	0.19 ± 0.07	0.08 ± 0.02
Protein binding ratio (%)	98.70 ± 0.56	99.54 ± 0.19

[a] Atotal is defined as the amount of total F-53B in the plasma (before ultrafiltration centrifugation).

[b] Afree is defined as the amount of unbound F-53B in plasma (after ultrafiltration centrifugation).

Table S12

Pharmacokinetic Parameters of F-53B following oral or IV administration in pregnant mice [a]

Parameter [b]	Oral [c]	IV
C_{max} (μg/mL)	0.25 ± 0.02	0.37 ± 0.08
T_{max} (h)	24.00	8.00
$t_{1/2}$ (h)	154.00 ± 2.44	81.59 ± 2.61
AUC_{0-96} (h*μg/mL)	13.82 ± 1.24	24.60 ± 2.64
$AUC_{0-\infty}$ (h*μg/mL)	49.13 ± 40.14	61.22 ± 41.81
CL (mL/h/kg)	2.33 ± 1.21	1.82 ± 1.08
V_d (mL/kg)	452.68 ± 98.33	201.92 ± 48.86
Bioavailability	0.78	

[a] Each value represents the mean ± SEM (n=4).

[b] C_{max}, the maximum plasma concentration; T_{max}, the time to reach C_{max}; $t_{1/2}$, the elimination half-life; AUC_{0-96}, the area under the concentration-time curve from zero to 96 hours after administration; $AUC_{0-\infty}$, the area under the concentration-time curve from zero to infinity; CL, clearance; V_d, the volume of distribution; Bioavailability, absolute bioavailability.

[c] The volume of distribution and clearance were calculated as CL/F and Vd/F, where F is the fraction of absorbed dose.

Table S13

Sensitive parameters identified by the local sensitivity analysis[a]

Parameters[b]	Normalized sensitivity coefficients (NSCs)							
	Mice-Gestation						Human-Gestation	
	Maternal Plasma	Maternal Liver	Placenta	Fetal Plasma	Fetal Liver	Fetal Brain	Maternal Plasma	Fetal Plasma
BW	-0.8925	-0.8918	-0.8928	-0.9016	-0.8069	-0.8759	-0.7031	-0.7025
Free	-0.0436	-0.0485	0.0865	0.1068	0.1208	0.1148	-0.2313	0.7672
Free_Fet	-0.0733	-0.0729	-0.1773	-0.1865	0.5193	0.2361	0.0103	-0.9473
GEC	0.0277	0.0275	0.0693	0.0746	0.5419	0.1925	0.0014	0.0009
GFRC	0.0271	0.0270	0.0687	0.0740	0.5404	0.1915	<1e-5	<1e-5
Htc	0.1096	0.1138	0.1175	0.1287	-0.0969	-0.1643	<1e-5	<1e-5
K0C	0.0295	0.0294	0.0721	0.0777	0.5523	0.1980	0.0022	0.0017
Kabsc	<1e-5	<1e-5	<1e-5	<1e-5	<1e-5	<1e-5	<1e-5	<1e-5
KbileC	0.0072	0.0071	0.0191	0.0205	0.1574	0.0550	-0.0001	-0.0001
Kdif	0.0170	0.0169	0.0449	0.0485	0.3635	0.1275	0.0161	0.0157
KeffluxC	0.0459	0.0457	0.0877	0.0933	0.5559	0.2094	0.1675	0.1675
Km_apical	0.0271	0.0269	0.0687	0.0741	0.5381	0.1910	-0.0042	-0.0043
Km_baso	0.0170	0.0169	0.0442	0.0476	0.3500	0.1236	0.0737	0.0741
Ktrans1C	-0.0820	-0.0814	-0.1924	0.8158	0.9098	0.8358	-0.1139	0.8821
Ktrans2C	0.0829	0.0823	0.2035	-0.7775	-0.7207	-0.7595	0.087	-0.6471
Ktrans3C	-0.0160	-0.0158	-0.0228	-0.0246	-0.0619	-0.0362	-0.0722	-0.289
Ktrans4C	0.0029	0.0029	0.0042	0.0046	0.0111	0.0068	0.0155	0.0577
KunabsC	0.0329	0.0327	0.0795	0.0857	0.6046	0.2174	-0.0002	-0.0002
KurineC	-0.0001	-0.0001	-0.0001	-0.0001	-0.0001	-0.0001	-0.0034	-0.0034

PB_Fet	-0.0008	-0.0008	-0.0044	-0.0045	-0.0060	0.5722	<1e-5	<1e-5
PF	-0.0079	-0.0078	0.0336	0.0385	0.5072	0.1570	-0.1620	-0.1625
PK	<1e-5	<1e-5	<1e-5	<1e-5	<1e-5	<1e-5	<1e-5	<1e-5
PL	-0.1980	0.8010	-0.1560	-0.1528	0.3410	-0.0278	-0.0912	-0.091
PL_Fet	0.0242	0.0241	0.0607	0.0656	0.8547	0.1829	-0.0032	-0.0155
PM	0.0244	0.0243	0.0660	0.0712	0.5379	0.1888	-0.0026	-0.0026
PPla	0.0344	0.0342	1.0812	0.0872	0.6585	0.2318	0.001	0.0005
PRest	-0.5959	-0.5929	-0.5981	-0.6043	-0.5633	-0.5921	-0.4323	-0.4324
PRest_Fet	-0.0012	-0.0012	-0.0014	-0.0014	-0.0042	-0.0021	-0.0072	-0.0280
protein	0.0256	0.0255	0.0673	0.0728	0.5368	0.1897	-0.0672	-0.0676
QBC_Fet	0.0104	0.0103	0.0301	0.0321	0.1187	0.4720	-[c]	-
QC_Fet	<1e-5	<1e-5	<1e-5	<1e-5	<1e-5	<1e-5	-0.0539	-0.0521
QC_P	<1e-5	<1e-5	<1e-5	<1e-5	<1e-5	<1e-5	-	-
QF_P	<1e-5	<1e-5	<1e-5	<1e-5	<1e-5	<1e-5	<1e-5	<1e-5
QFC	0.0270	0.0269	0.0686	0.0739	0.5401	0.1912	<1e-5	<1e-5
QKC	-0.0188	-0.0187	-0.0187	-0.0188	-0.0163	-0.0181	<1e-5	<1e-5
QLC	0.0287	0.0235	0.0698	0.0752	0.5338	0.1915	<1e-5	<1e-5
QLC_Fet	0.0384	0.0382	0.0958	0.1032	1.3021	0.2343	-	-
QM_P	<1e-5	<1e-5	<1e-5	<1e-5	<1e-5	<1e-5	-	-
QMC	0.0152	0.0151	0.0401	0.0431	0.3185	0.1117	0.0018	0.0012
QPla	<1e-5	<1e-5	<1e-5	<1e-5	<1e-5	<1e-5	<1e-5	<1e-5
RAFapi	0.0009	0.0009	0.0010	0.0011	0.0000	0.0009	0.0042	0.0042
RAFbaso	0.0001	0.0001	0.0004	0.0005	0.0004	0.0005	-0.0713	-0.0718
VAm	<1e-5	<1e-5	<1e-5	<1e-5	<1e-5	<1e-5	<1e-5	<1e-5
VB_Fet	<1e-5	<1e-5	<1e-5	<1e-5	<1e-5	<1e-5	<1e-5	<1e-5
VF_P	<1e-5	<1e-5	<1e-5	<1e-5	<1e-5	<1e-5	<1e-5	<1e-5
VFC	0.0295	0.0294	0.0446	0.0467	0.2128	0.0879	0.1611	0.160

VFet	<1e-5	<1e-5	<1e-5	<1e-5	<1e-5	<1e-5	<1e-5	<1e-5
VFilC	0.0271	0.0269	0.0687	0.0741	0.5381	0.1910	-0.0042	-0.0043
VKC	0.0409	0.0407	0.0827	0.0883	0.5517	0.2050	-0.0783	-0.0798
VL_Fet	<1e-5	<1e-5	<1e-5	<1e-5	<1e-5	<1e-5	<1e-5	<1e-5
VLC	-0.1797	-0.1788	-0.1798	-0.1815	-0.1630	-0.1769	-0.0728	-0.0725
VM_P	<1e-5	<1e-5	<1e-5	<1e-5	<1e-5	<1e-5	<1e-5	<1e-5
Vmax_apical_invitro	0.0009	0.0009	0.0010	0.0011	2.0131e-5	0.0009	0.0042	0.0042
Vmax_baso_invitro	0.0323	0.0322	0.0793	0.0854	0.6063	0.2170	-0.0713	-0.0718
VMC	0.0323	0.0321	0.0739	0.0794	0.5426	0.1962	0.0044	0.004
VPla	<1e-5	<1e-5	<1e-5	<1e-5	<1e-5	<1e-5	<1e-5	<1e-5
VPlas	<1e-5	<1e-5	<1e-5	<1e-5	<1e-5	<1e-5	<1e-5	<1e-5
VPlasC	0.0621	0.0618	0.1039	0.1096	0.5706	0.2259	-	-
VPlasC_Fet	0.0280	0.0279	0.0730	0.0789	0.5849	0.2059	-	-
VPTCC	<1e-5	<1e-5	<1e-5	<1e-5	<1e-5	<1e-5	-0.0116	-0.0126

[a] The method of local sensitivity analysis is described in the manuscript.

[b] All parameters are defined in Table S3.

[c]"-" indicates that the parameter was not used in a specific model, and thus was not evaluated on dose metrics related to this specific model.

9. Supplementary Figures

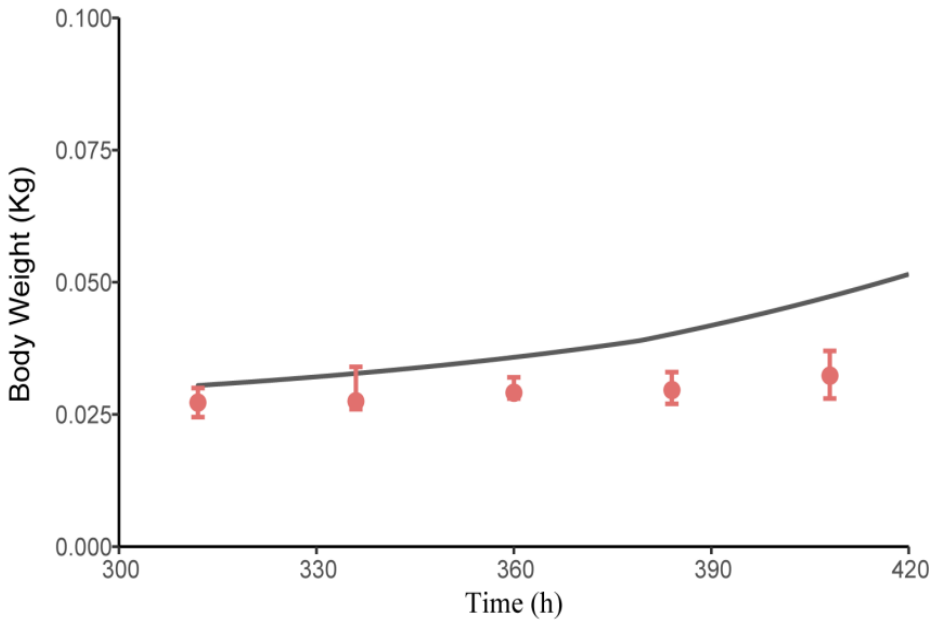

Figure S1. Plot of simulated values of growth equations (grey line) versus experimental values of body weight (pink circles, mean [range]).

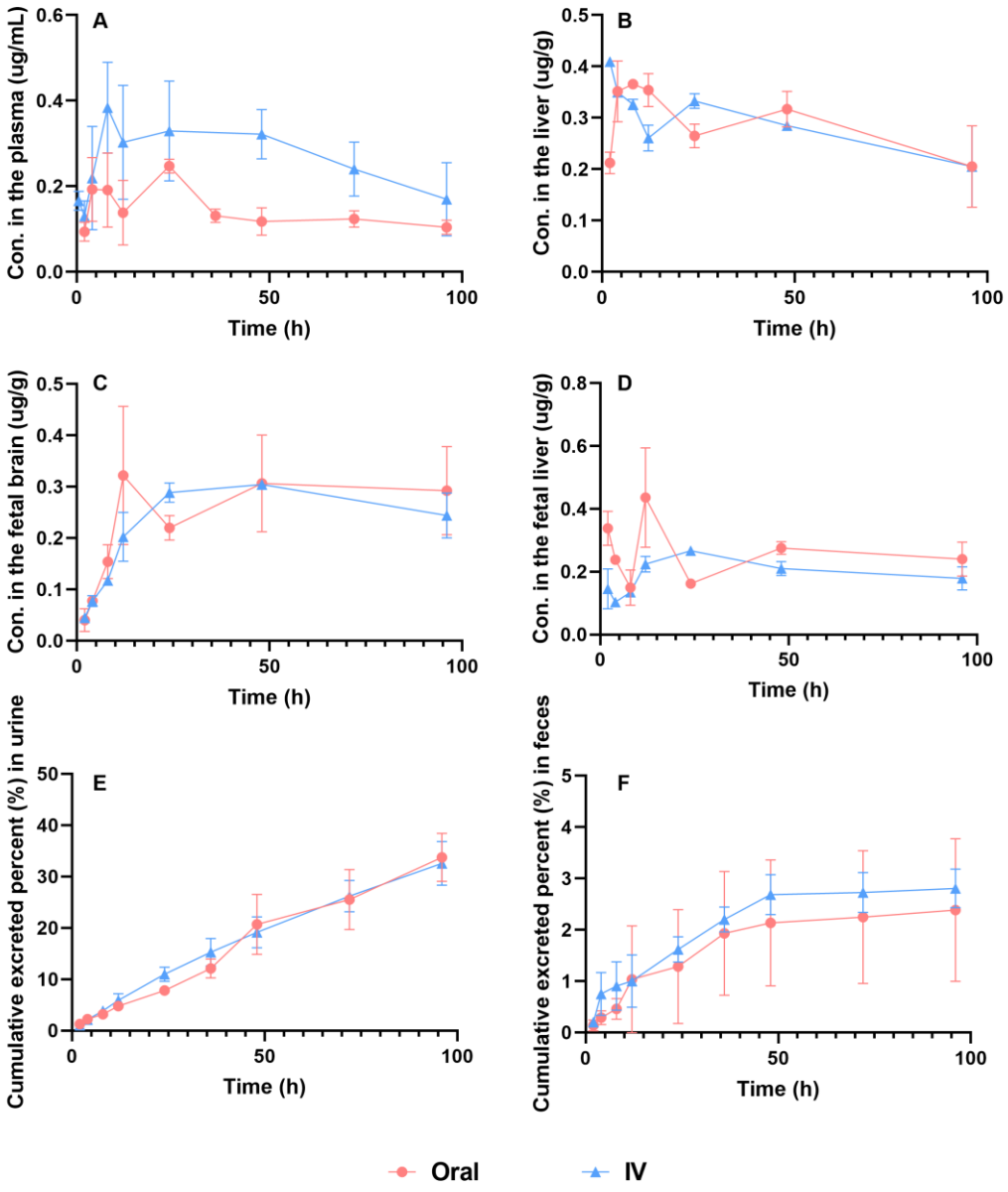

Figure S2. Experimental concentration (mean ± SD) of F-53B via oral and IV administrations in maternal plasma (A), maternal liver (B), fetal brain (C) and fetal liver (D). Comparisons of cumulative excreted percent (%) of F-53B in urine (E) and feces (F).

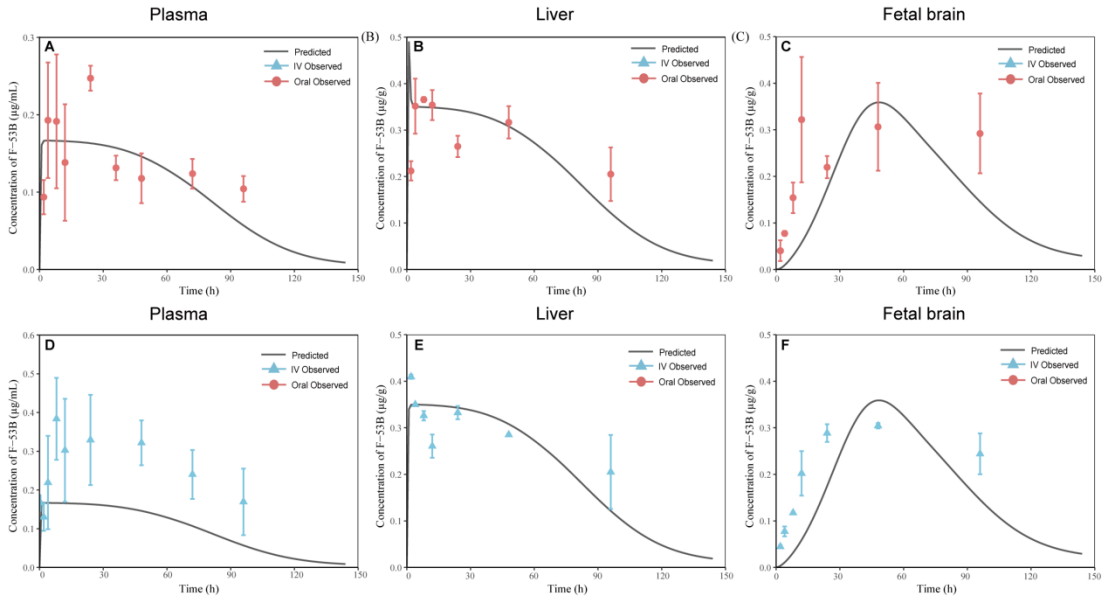

Figure S3. Fitting plot between model predictions and observed values. Comparison of plasma, liver, and fetal brain concentrations (mean ± SD) after oral exposure (A-C) and IV exposure (D-G) of 80 μg/kg of F-53B with model predictions (lines). In the plot, the Time indicates the time after exposure (e.g., 0h refers to gestational day 13).

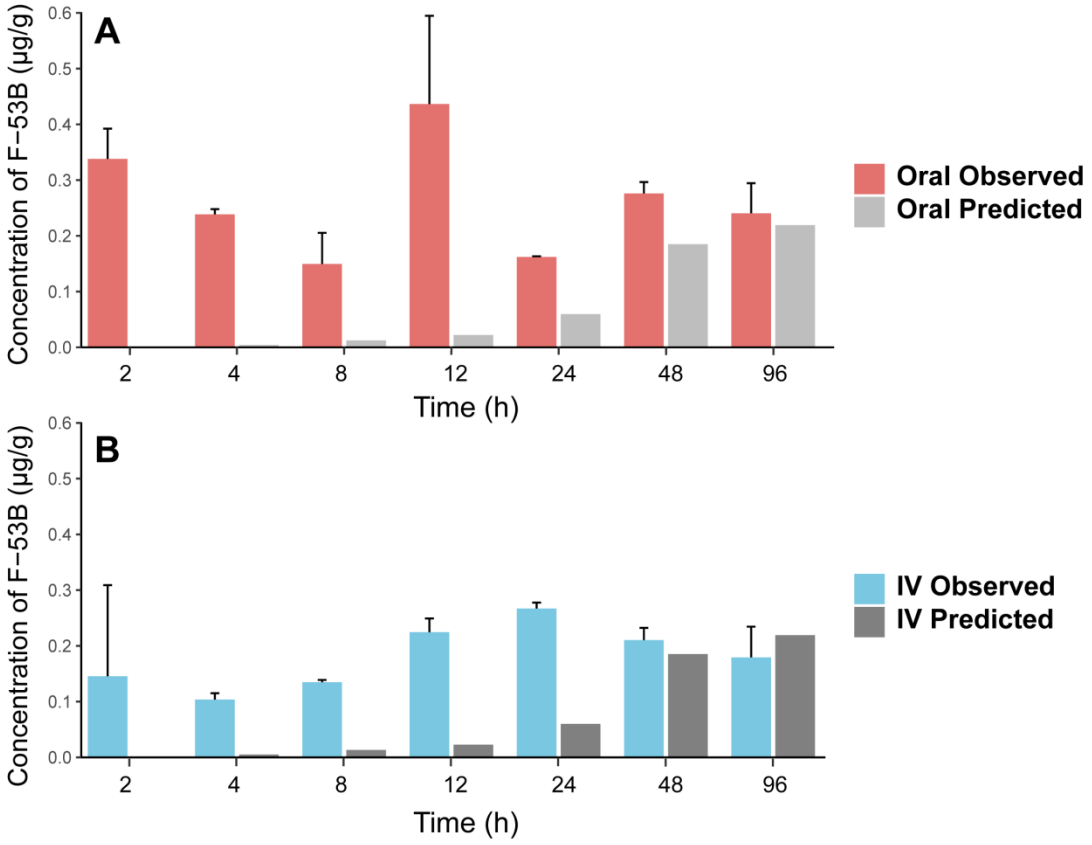

Figure S4. Comparison of model predictions of fetal liver with in-house experimental data (mean ± SD) after oral (A) and IV (B) administrations.

Note: IV, intravenous; SD: standard deviation.

10. Supplementary References

(1) Liang, L. X.; Liang, J.; Li, Q. Q.; Zeeshan, M.; Zhang, Z.; Jin, N.; Lin, L. Z.; Wu, L. Y.; Sun, M. K.; Tan, W. H.; Zhou, Y.; Chu, C.; Hu, L. W.; Liu, R. Q.; Zeng, X. W.; Yu, Y.; Dong, G. H. Early Life Exposure to F-53B Induces Neurobehavioral Changes in Developing Children and Disturbs Dopamine-Dependent Synaptic Signaling in Weaning Mice. *Environ Int* **2023**, *181*, 108272. https://doi.org/10.1016/j.envint.2023.108272.

(2) Lai, K. P.; Lee, J. C.; Wan, H. T.; Li, J. W.; Wong, A. Y.; Chan, T. F.; Oger, C.; Galano, J. M.; Durand, T.; Leung, K. S.; Leung, C. C.; Li, R.; Wong, C. K. Effects of in Utero PFOS Exposure on Transcriptome, Lipidome, and Function of Mouse Testis. *Environ Sci Technol* **2017**, *51* (15), 8782–8794. https://doi.org/10.1021/acs.est.7b02102.

(3) EPA. *EPA Non-Regulatory Health-Based Drinking Water Levels | US EPA*. https://www.epa.gov/sdwa/epa-non-regulatory-health-based-drinking-water-levels.

(4) Shi, Y.; Vestergren, R.; Xu, L.; Zhou, Z.; Li, C.; Liang, Y.; Cai, Y. Human Exposure and Elimination Kinetics of Chlorinated Polyfluoroalkyl Ether Sulfonic Acids (Cl-PFESAs). *Environ Sci Technol* **2016**, *50* (5), 2396–2404. https://doi.org/10.1021/acs.est.5b05849.

(5) Wang, Y.; Shi, Y.; Vestergren, R.; Zhou, Z.; Liang, Y.; Cai, Y. Using Hair, Nail and Urine Samples for Human Exposure Assessment of Legacy and Emerging per- and Polyfluoroalkyl Substances. *Sci Total Environ* **2018**, *636*, 383–391. https://doi.org/10.1016/j.scitotenv.2018.04.279.

(6) Chu, C.; Zhou, Y.; Li, Q. Q.; Bloom, M. S.; Lin, S.; Yu, Y. J.; Chen, D.; Yu, H. Y.; Hu, L. W.; Yang, B. Y.; Zeng, X. W.; Dong, G. H. Are Perfluorooctane Sulfonate Alternatives Safer? New Insights from a Birth Cohort Study. *Environ Int* **2020**, *135*, 105365. https://doi.org/10.1016/j.envint.2019.105365.

(7) Jeong, S. H.; Jang, J. H.; Cho, H. Y.; Lee, Y. B. Risk Assessment for Humans Using Physiologically Based Pharmacokinetic Model of Diethyl Phthalate and Its Major Metabolite, Monoethyl Phthalate. *Arch Toxicol* **2020**, *94* (7), 2377–2400.

https://doi.org/10.1007/s00204-020-02748-9.

(8) Kim, S. J.; Shin, H.; Lee, Y. B.; Cho, H. Y. Sex-Specific Risk Assessment of PFHxS Using a Physiologically Based Pharmacokinetic Model. *Arch Toxicol* **2018**, *92* (3), 1113–1131. https://doi.org/10.1007/s00204-017-2116-5.

(9) Worley, R. R.; Fisher, J. Application of Physiologically-Based Pharmacokinetic Modeling to Explore the Role of Kidney Transporters in Renal Reabsorption of Perfluorooctanoic Acid in the Rat. *Toxicol Appl Pharmacol* **2015**, *289* (3), 428–441. https://doi.org/10.1016/j.taap.2015.10.017.

(10) Chou, W. C.; Lin, Z. Bayesian Evaluation of a Physiologically Based Pharmacokinetic (PBPK) Model for Perfluorooctane Sulfonate (PFOS) to Characterize the Interspecies Uncertainty between Mice, Rats, Monkeys, and Humans: Development and Performance Verification. *Environ Int* **2019**, *129*, 408–422. https://doi.org/10.1016/j.envint.2019.03.058.

(11) Chou, W. C.; Lin, Z. Development of a Gestational and Lactational Physiologically Based Pharmacokinetic (PBPK) Model for Perfluorooctane Sulfonate (PFOS) in Rats and Humans and Its Implications in the Derivation of Health-Based Toxicity Values. *Environ Health Perspect* **2021**, *129* (3), 37004. https://doi.org/10.1289/EHP7671.

(12) Lau, C.; Rumpler, J.; Das, K. P.; Wood, C. R.; Schmid, J. E.; Strynar, M. J.; Wambaugh, J. F. Pharmacokinetic Profile of Perfluorobutane Sulfonate and Activation of Hepatic Nuclear Receptor Target Genes in Mice. *Toxicology* **2020**, *441*, 152522. https://doi.org/10.1016/J.TOX.2020.152522.

(13) Yi, S.; Yang, D.; Zhu, L.; Mabury, S. A. Significant Reductive Transformation of 6:2 Chlorinated Polyfluorooctane Ether Sulfonate to Form Hydrogen-Substituted Polyfluorooctane Ether Sulfonate and Their Toxicokinetics in Male Sprague-Dawley Rats. *Environ Sci Technol* **2022**, *56* (10), 6123–6132. https://doi.org/10.1021/acs.est.1c00616.

(14) Lappin, G.; Rowland, M.; Garner, R. C. The Use of Isotopes in the Determination of Absolute Bioavailability of Drugs in Humans. *Expert Opin Drug Metab Toxicol* **2006**,

2 (3), 419–427. https://doi.org/10.1517/17425255.2.3.419.

(15) Lin, Z.; Fisher, J. W.; Ross, M. K.; Filipov, N. M. A Physiologically Based Pharmacokinetic Model for Atrazine and Its Main Metabolites in the Adult Male C57BL/6 Mouse. *Toxicol Appl Pharmacol* **2011**, *251* (1), 16–31. https://doi.org/10.1016/j.taap.2010.11.009.

(16) Worley, R. R.; Yang, X.; Fisher, J. Physiologically Based Pharmacokinetic Modeling of Human Exposure to Perfluorooctanoic Acid Suggests Historical Non Drinking-Water Exposures Are Important for Predicting Current Serum Concentrations. *Toxicol Appl Pharmacol* **2017**, *330*, 9–21. https://doi.org/10.1016/j.taap.2017.07.001.

(17) Haddad, S.; Restieri, C.; Krishnan, K. Characterization of Age-Related Changes in Body Weight and Organ Weights from Birth to Adolescence in Humans. *J Toxicol Environ Health A* **2001**, *64* (6), 453–464. https://doi.org/10.1080/152873901753215911.

(18) Yang, X.; Doerge, D. R.; Fisher, J. W. Prediction and Evaluation of Route Dependent Dosimetry of BPA in Rats at Different Life Stages Using a Physiologically Based Pharmacokinetic Model. *Toxicol Appl Pharmacol* **2013**, *270* (1), 45–59. https://doi.org/10.1016/j.taap.2013.03.022.

(19) Yang, X.; Doerge, D. R.; Teeguarden, J. G.; Fisher, J. W. Development of a Physiologically Based Pharmacokinetic Model for Assessment of Human Exposure to Bisphenol A. *Toxicol Appl Pharmacol* **2015**, *289* (3), 442–456. https://doi.org/10.1016/j.taap.2015.10.016.

(20) Qi, Z.; Whitt, I.; Mehta, A.; Jin, J.; Zhao, M.; Harris, R. C.; Fogo, A. B.; Breyer, M. D. Serial Determination of Glomerular Filtration Rate in Conscious Mice Using FITC-Inulin Clearance. *Am J Physiol Renal Physiol* **2004**, *286* (3), F590-6. https://doi.org/10.1152/ajprenal.00324.2003.

(21) Hejtmancik, M. R.; Ryan, M. J.; Toft, J. D.; Persing, R. L.; Kurtz, P. J.; Chhabra, R. S. Hematological Effects in F344 Rats and B6C3F1 Mice during the 13-Week Gavage Toxicity Study of Methylene Blue Trihydrate. *Toxicol Sci* **2002**, *65* (1), 126–

134. https://doi.org/10.1093/toxsci/65.1.126.

(22) Davies, B.; Morris, T. Physiological Parameters in Laboratory Animals and Humans. *Pharm Res* **1993**, *10* (7), 1093–1095. https://doi.org/10.1023/a:1018943613122.

(23) Addis, T.; Poo, L. J.; Lew, W. The Quantities of Protein Lost by the Various Organs and Tissues of the Body during a Fast. *Journal of Biological Chemistry* **1936**, *115* (1), 111–116. https://doi.org/10.1016/s0021-9258(18)74756-x.

(24) Hsu, V.; De L. T. Vieira, M.; Zhao, P.; Zhang, L.; Zheng, J. H.; Nordmark, A.; Berglund, E. G.; Giacomini, K. M.; Huang, S.-M. Towards Quantitation of the Effects of Renal Impairment and Probenecid Inhibition on Kidney Uptake and Efflux Transporters, Using Physiologically Based Pharmacokinetic Modelling and Simulations. *Clin Pharmacokinet* **2014**, *53* (3), 283–293. https://doi.org/10.1007/s40262-013-0117-y.

(25) Brown, R. P.; Delp, M. D.; Lindstedt, S. L.; Rhomberg, L. R.; Beliles, R. P. Physiological Parameter Values for Physiologically Based Pharmacokinetic Models. *Toxicol Ind Health* **1997**, *13* (4), 407–484. https://doi.org/10.1177/074823379701300401.

(26) Loccisano, A. E.; Campbell Jr., J. L.; Butenhoff, J. L.; Andersen, M. E.; Clewell 3rd, H. J. Evaluation of Placental and Lactational Pharmacokinetics of PFOA and PFOS in the Pregnant, Lactating, Fetal and Neonatal Rat Using a Physiologically Based Pharmacokinetic Model. *Reprod Toxicol* **2012**, *33* (4), 468–490. https://doi.org/10.1016/j.reprotox.2011.07.003.

(27) Yoon, M.; Nong, A.; Clewell, H. J.; Taylor, M. D.; Dorman, D. C.; Andersen, M. E. Evaluating Placental Transfer and Tissue Concentrations of Manganese in the Pregnant Rat and Fetuses after Inhalation Exposures with a PBPK Model. *Toxicological Sciences* **2009**, *112* (1), 44–58. https://doi.org/10.1093/toxsci/kfp198.

(28) Hanwell, A.; Linzell, J. L. The Time Course of Cardiovascular Changes in Lactation in the Rat. *J Physiol* **1973**, *233* (1), 93–109.

https://doi.org/10.1113/jphysiol.1973.sp010299.

(29) Yoon, M.; Schroeter, J. D.; Nong, A.; Taylor, M. D.; Dorman, D. C.; Andersen, M. E.; Clewell 3rd, H. J. Physiologically Based Pharmacokinetic Modeling of Fetal and Neonatal Manganese Exposure in Humans: Describing Manganese Homeostasis during Development. *Toxicol Sci* **2011**, *122* (2), 297–316. https://doi.org/10.1093/toxsci/kfr141.

(30) Carter, A. M.; Gu, W. Cerebral Blood Flow in the Fetal Guinea-Pig. *J Dev Physiol* **1988**, *10* (2), 123–129.

(31) Kapraun, D. F.; Wambaugh, J. F.; Setzer, R. W.; Judson, R. S. Empirical Models for Anatomical and Physiological Changes in a Human Mother and Fetus during Pregnancy and Gestation. *PLoS One* **2019**, *14* (5), e0215906. https://doi.org/10.1371/journal.pone.0215906.

(32) O'Flaherty, E. J.; Scott, W.; Schreiner, C.; Beliles, R. P. A Physiologically Based Kinetic Model of Rat and Mouse Gestation: Disposition of a Weak Acid. *Toxicol Appl Pharmacol* **1992**, *112* (2), 245–256. https://doi.org/10.1016/0041-008x(92)90194-w.

(33) Clarke, D. O.; Elswick, B. A.; Welsch, F.; Conolly, R. B. Pharmacokinetics of 2-Methoxyethanol and 2-Methoxyacetic Acid in the Pregnant Mouse: A Physiologically Based Mathematical Model. *Toxicol Appl Pharmacol* **1993**, *121* (2), 239–252. https://doi.org/10.1006/taap.1993.1151.

(34) Crowell, S. R.; Sharma, A. K.; Amin, S.; Soelberg, J. J.; Sadler, N. C.; Wright, A. T.; Baird, W. M.; Williams, D. E.; Corley, R. A. Impact of Pregnancy on the Pharmacokinetics of Dibenzo[Def,p]Chrysene in Mice. *Toxicol Sci* **2013**, *135* (1), 48–62. https://doi.org/10.1093/toxsci/kft124.

(35) O'Flaherty, E. J.; Nau, H.; McCandless, D.; Beliles, R. P.; Schreiner, C. M.; Scott Jr., W. J. Physiologically Based Pharmacokinetics of Methoxyacetic Acid: Dose-Effect Considerations in C57BL/6 Mice. *Teratology* **1995**, *52* (2), 78–89. https://doi.org/10.1002/tera.1420520204.

(36) Ward, K. W.; Blumenthal, G. M.; Welsch, F.; Pollack, G. M. Development of a

Physiologically Based Pharmacokinetic Model to Describe the Disposition of Methanol in Pregnant Rats and Mice. *Toxicol Appl Pharmacol* **1997**, *145* (2), 311–322. https://doi.org/10.1006/taap.1997.8170.

(37) Clewell, R. A.; Kremer, J. J.; Williams, C. C.; Campbell Jr., J. L.; Andersen, M. E.; Borghoff, S. J. Tissue Exposures to Free and Glucuronidated Monobutylyphthalate in the Pregnant and Fetal Rat Following Exposure to Di-n-Butylphthalate: Evaluation with a PBPK Model. *Toxicol Sci* **2008**, *103* (2), 241–259. https://doi.org/10.1093/toxsci/kfn054.

(38) Wykoff, M. H. Weight Changes of the Developing Rat Conceptus. *Am J Vet Res* **1971**, *32* (10), 1633–1635.

(39) Sikov, M. R.; Thomas, J. M. Prenatal Growth of the Rat. *Growth* **1970**, *34* (1), 1–14.

(40) Loccisano, A. E.; Longnecker, M. P.; Campbell Jr., J. L.; Andersen, M. E.; Clewell 3rd, H. J. Development of PBPK Models for PFOA and PFOS for Human Pregnancy and Lactation Life Stages. *J Toxicol Environ Health A* **2013**, *76* (1), 25–57. https://doi.org/10.1080/15287394.2012.722523.

(41) Abduljalil, K.; Furness, P.; Johnson, T. N.; Rostami-Hodjegan, A.; Soltani, H. Anatomical, Physiological and Metabolic Changes with Gestational Age during Normal Pregnancy: A Database for Parameters Required in Physiologically Based Pharmacokinetic Modelling. *Clin Pharmacokinet* **2012**, *51* (6), 365–396. https://doi.org/10.2165/11597440-000000000-00000.

(42) Gentry, P. R.; Covington, T. R.; Clewell 3rd, H. J. Evaluation of the Potential Impact of Pharmacokinetic Differences on Tissue Dosimetry in Offspring during Pregnancy and Lactation. *Regul Toxicol Pharmacol* **2003**, *38* (1), 1–16. https://doi.org/10.1016/s0273-2300(03)00047-3.

(43) Valentin J, S. C. Basic Anatomical and Physiological Data for Use in Radiological Protection: Reference Values. A Report of Age- and Gender-Related Differences in the Anatomical and Physiological Characteristics of Reference Individuals. ICRP

Publication 89. *Ann ICRP* **2002**, *32* (3–4), 5–265.

(44) Clewell, H. J.; Gearhart, J. M.; Gentry, P. R.; Covington, T. R.; VanLandingham, C. B.; Crump, K. S.; Shipp, A. M. Evaluation of the Uncertainty in an Oral Reference Dose for Methylmercury Due to Interindividual Variability in Pharmacokinetics. *Risk Anal* **1999**, *19* (4), 547–558. https://doi.org/10.1023/a:1007017116171.

(45) Overmoyer, B. A.; McLaren, C. E.; Brittenham, G. M. Uniformity of Liver Density and Nonheme (Storage) Iron Distribution. *Arch Pathol Lab Med* **1987**, *111* (6), 549–554.

(46) Wang, Y.; Li, X.; Zheng, Z.; Shi, Y.; Cai, Y. Chlorinated Polyfluoroalkyl Ether Sulfonic Acids in Fish, Dust, Drinking Water and Human Serum: From External Exposure to Internal Doses. *Environ Int* **2021**, *157*. https://doi.org/10.1016/j.envint.2021.106820.

(47) Jin, Q.; Shi, Y.; Cai, Y. Occurrence and Risk of Chlorinated Polyfluoroalkyl Ether Sulfonic Acids (Cl-PFESAs) in Seafood from Markets in Beijing, China. *Science of The Total Environment* **2020**, *726*. https://doi.org/10.1016/j.scitotenv.2020.138538.

(48) Chen, X.; Feng, X.; Sun, X.; Li, Y.; Yang, Y.; Shan, G.; Zhu, L. Quantifying Indirect Contribution from Precursors to Human Body Burden of Legacy PFASs Based on Paired Blood and One-Week Duplicate Diet. *Environ Sci Technol* **2022**, *56* (9), 5632–5640. https://doi.org/10.1021/acs.est.1c07465.

(49) Sun, Q.; Bi, R.; Wang, T.; Su, C.; Chen, Z.; Diao, J.; Zheng, Z.; Liu, W. Are There Risks Induced by Novel and Legacy Poly- and Perfluoroalkyl Substances in Coastal Aquaculture Base in South China. *Science of The Total Environment* **2021**, *779*. https://doi.org/10.1016/j.scitotenv.2021.146539.

(50) Wang, Y.; Gao, X.; Liu, J.; Lyu, B.; Li, J.; Zhao, Y.; Wu, Y. Exposure to Emerging and Legacy Polyfluoroalkyl Substances in the Sixth Total Diet Study - China, 2016-2019. *China CDC Wkly* **2022**, *4* (9), 168–171. https://doi.org/10.46234/ccdcw2022.042.

(51) Pan, Y.; Zhu, Y.; Zheng, T.; Cui, Q.; Buka, S. L.; Zhang, B.; Guo, Y.; Xia, W.; Yeung, L. W.; Li, Y.; Zhou, A.; Qiu, L.; Liu, H.; Jiang, M.; Wu, C.; Xu, S.; Dai, J. Novel

Chlorinated Polyfluorinated Ether Sulfonates and Legacy Per-/Polyfluoroalkyl Substances: Placental Transfer and Relationship with Serum Albumin and Glomerular Filtration Rate. *Environ Sci Technol* **2017**, *51* (1), 634–644. https://doi.org/10.1021/acs.est.6b04590.

(52) Chen, F.; Yin, S.; Kelly, B. C.; Liu, W. Chlorinated Polyfluoroalkyl Ether Sulfonic Acids in Matched Maternal, Cord, and Placenta Samples: A Study of Transplacental Transfer. *Environ Sci Technol* **2017**, *51* (11), 6387–6394. https://doi.org/10.1021/acs.est.6b06049.

(53) Gao, K.; Zhuang, T.; Liu, X.; Fu, J.; Zhang, J.; Fu, J.; Wang, L.; Zhang, A.; Liang, Y.; Song, M.; Jiang, G. Prenatal Exposure to Per- and Polyfluoroalkyl Substances (PFASs) and Association between the Placental Transfer Efficiencies and Dissociation Constant of Serum Proteins-PFAS Complexes. *Environ Sci Technol* **2019**, *53* (11), 6529–6538. https://doi.org/10.1021/acs.est.9b00715.

(54) Xu, C.; Yin, S.; Liu, Y.; Chen, F.; Zhong, Z.; Li, F.; Liu, K.; Liu, W. Prenatal Exposure to Chlorinated Polyfluoroalkyl Ether Sulfonic Acids and Perfluoroalkyl Acids: Potential Role of Maternal Determinants and Associations with Birth Outcomes. *J Hazard Mater* **2019**, *380*, 120867. https://doi.org/10.1016/j.jhazmat.2019.120867.

(55) Cai, D.; Li, Q. Q.; Chu, C.; Wang, S. Z.; Tang, Y. T.; Appleton, A. A.; Qiu, R. L.; Yang, B. Y.; Hu, L. W.; Dong, G. H.; Zeng, X. W. High Trans-Placental Transfer of Perfluoroalkyl Substances Alternatives in the Matched Maternal-Cord Blood Serum: Evidence from a Birth Cohort Study. *Sci Total Environ* **2020**, *705*, 135885. https://doi.org/10.1016/j.scitotenv.2019.135885.

(56) Wang, J.; Pan, Y.; Wei, X.; Dai, J. Temporal Trends in Prenatal Exposure (1998-2018) to Emerging and Legacy Per- and Polyfluoroalkyl Substances (PFASs) in Cord Plasma from the Beijing Cord Blood Bank, China. *Environ Sci Technol* **2020**, *54* (20), 12850–12859. https://doi.org/10.1021/acs.est.0c01877.

(57) Li, Y.; Lu, X.; Yu, N.; Li, A.; Zhuang, T.; Du, L.; Tang, S.; Shi, W.; Yu, H.; Song, M.; Wei, S. Exposure to Legacy and Novel Perfluoroalkyl Substance Disturbs the

Metabolic Homeostasis in Pregnant Women and Fetuses: A Metabolome-Wide Association Study. *Environ Int* **2021**, *156*, 106627. https://doi.org/10.1016/j.envint.2021.106627.

(58) Liu, Y.; Li, A.; An, Q.; Liu, K.; Zheng, P.; Yin, S.; Liu, W. Prenatal and Postnatal Transfer of Perfluoroalkyl Substances from Mothers to Their Offspring. *Crit Rev Environ Sci Technol* **2021**, *52* (14), 2510–2537. https://doi.org/10.1080/10643389.2021.1886556.

(59) Xia, X.; Zheng, Y.; Tang, X.; Zhao, N.; Wang, B.; Lin, H.; Lin, Y. Nontarget Identification of Novel Per- and Polyfluoroalkyl Substances in Cord Blood Samples. *Environ Sci Technol* **2022**, *56* (23), 17061–17069. https://doi.org/10.1021/acs.est.2c04820.

(60) Zheng, P.; Liu, Y.; An, Q.; Yang, X.; Yin, S.; Ma, L. Q.; Liu, W. Prenatal and Postnatal Exposure to Emerging and Legacy Per-/Polyfluoroalkyl Substances: Levels and Transfer in Maternal Serum, Cord Serum, and Breast Milk. *Science of The Total Environment* **2022**, *812*. https://doi.org/10.1016/j.scitotenv.2021.152446.

(61) Zhang, B.; Wei, Z.; Gu, C.; Yao, Y.; Xue, J.; Zhu, H.; Kannan, K.; Sun, H.; Zhang, T. First Evidence of Prenatal Exposure to Emerging Poly- and Perfluoroalkyl Substances Associated with E-Waste Dismantling: Chemical Structure-Based Placental Transfer and Health Risks. *Environ Sci Technol* **2022**, *56* (23), 17108–17118. https://doi.org/10.1021/acs.est.2c05925.

(62) Cao, Z.; Li, J.; Yang, M.; Gong, H.; Xiang, F.; Zheng, H.; Cai, X.; Xu, S.; Zhou, A.; Xiao, H. Prenatal Exposure to Perfluorooctane Sulfonate Alternatives and Associations with Neonatal Thyroid Stimulating Hormone Concentration: A Birth Cohort Study. *Chemosphere* **2023**, *311* (Pt 1), 136940. https://doi.org/10.1016/j.chemosphere.2022.136940.

(63) Fan, Y.; Guo, L.; Wang, R.; Xu, J.; Fang, Y.; Wang, W.; Lv, J.; Tang, W.; Wang, H.; Xu, D.-X.; Tao, L.; Huang, Y. Low Transplacental Transfer of PFASs in the Small-for-Gestational-Age (SGA) New-Borns: Evidence from a Chinese Birth Cohort.

Chemosphere **2023**, *340*, 139964. https://doi.org/10.1016/j.chemosphere.2023.139964.
(64) Ji, D.; Pan, Y.; Qiu, X.; Gong, J.; Li, X.; Niu, C.; Yao, J.; Luo, S.; Zhang, Z.; Wang, Q.; Dai, J.; Wei, Y. Unveiling Distribution of Per- and Polyfluoroalkyl Substances in Matched Placenta-Serum Tetrads: Novel Implications for Birth Outcome Mediated by Placental Vascular Disruption. *Environ Sci Technol* **2023**, *57* (14), 5782–5793. https://doi.org/10.1021/acs.est.2c09184.
(65) Li, Q. Q.; Huang, J.; Cai, D.; Chou, W. C.; Zeeshan, M.; Chu, C.; Zhou, Y.; Lin, L.; Ma, H. M.; Tang, C.; Kong, M.; Xie, Y.; Dong, G. H.; Zeng, X. W. Prenatal Exposure to Legacy and Alternative Per- and Polyfluoroalkyl Substances and Neuropsychological Development Trajectories over the First 3 Years of Life. *Environ Sci Technol* **2023**, *57* (9), 3746–3757. https://doi.org/10.1021/acs.est.2c07807.
(66) Li, X.; Liu, H.; Wan, H.; Li, Y.; Xu, S.; Xiao, H.; Xia, W. Sex-Specific Associations between Legacy and Novel per- and Polyfluoroalkyl Substances and Telomere Length in Newborns in Wuhan, China: Mixture and Single Pollutant Associations. *Sci Total Environ* **2023**, *857* (Pt 3), 159676. https://doi.org/10.1016/j.scitotenv.2022.159676.
(67) Tian, Y.; Zhou, Q.; Zhang, L.; Li, W.; Yin, S.; Li, F.; Xu, C. In Utero Exposure to Per-/Polyfluoroalkyl Substances (PFASs): Preeclampsia in Pregnancy and Low Birth Weight for Neonates. *Chemosphere* **2023**, *313*, 137490. https://doi.org/10.1016/j.chemosphere.2022.137490.
(68) Zhang, Y.; Chen, R.; Gao, Y.; Qu, J.; Wang, Z.; Zhao, M.; Bai, X.; Jin, H. Human Serum Poly- and Perfluoroalkyl Substance Concentrations and Their Associations with Gestational Diabetes Mellitus. *Environ Pollut* **2023**, *317*, 120833. https://doi.org/10.1016/j.envpol.2022.120833.